

Flow Structure and Heat Transfer enhancement in Laminar Flow With Protrusion-Dimple Combinations in a Shallow Rectangular Channel

Author:

Alshroof, Osama; Reizes, John; Timchenko, Victoria; Leonardi, Eddie

Publication details:

Computational Heat Transfer

Event details:

ASME Summer Heat Transfer Conference
San Francisco, CA, USA

Publication Date:

2009

DOI:

<https://doi.org/10.26190/unsworks/625>

License:

<https://creativecommons.org/licenses/by-nc-nd/3.0/au/>

Link to license to see what you are allowed to do with this resource.

Downloaded from <http://hdl.handle.net/1959.4/41488> in <https://unsworks.unsw.edu.au> on 2024-03-28

HT2009-88251

FLOW STRUCTURE AND HEAT TRANSFER ENHANCEMENT IN LAMINAR FLOW WITH PROTRUSION-DIMPLE COMBINATIONS IN A SHALLOW RECTANGULAR CHANNEL

O. Alshroof*, J. Reizes, V. Timchenko and E. Leonardi

The University of New South Wales,
School of Mechanical and Manufacturing Engineering,
Sydney NSW, Australia 2052.

*Correspondence author. Fax: +61 2 9663 1222 Email: o.alshroof@unswalumni.com

ABSTRACT

The effect of introducing combinations of spherical dimples and protrusions in a shallow rectangular channel on the flow and heat transfer in the laminar regime has been studied numerically.

Four different cases were investigated. These consisted of: an isolated dimple, an isolated protrusion both placed on the centerline of one of the wide face of the channel, a combination of a dimple located on the centerline of the wide face of the channel and a protrusion located downstream but shifted to the side, and finally, a combination in which the protrusion and the dimple are reversed. The resultant, very complex flow structure and thermal fields in the channel are presented.

The introduction of a single dimple results in a small enhancement of heat transfer and a very small reduction in pressure drop relative to those obtained in a smooth channel. However, a significant enhancement in heat transfer obtained from a single protrusion is associated with marginal increase in pressure drop. The addition of a protrusion downstream of the dimple leads to an increase of 30% in heat transfer augmentation above that which pertains for the isolated protrusion without any increase in the pressure drop. With the reversal of the positions of the protrusion and the dimple no effect on either the pressure drop or the heat transfer has been observed.

KEYWORDS: Dimple, Protrusion, Heat Transfer Enhancement, Numerical Modeling.

INTRODUCTION

Both environmental and cost issues regarding energy usage, result in a pressing need to conserve energy. Therefore,

many researchers have attempted to develop new techniques for enhancing the effectiveness of heat transfer in the heat exchangers, thereby improving the performance of many devices (such as; air conditioning plants, through power stations, to computers). Unfortunately, an increase in the rate of heat transfer is usually accompanied by a concomitant increase in pressure drop, minimising the performance of heat exchangers, [1].

One method of heat transfer enhancement without introducing an unacceptable pressure drop penalty is to introduce dimpled and/or protruded surfaces [2, 3]. In fact, in a plate heat exchanger in which dimples are produced by a pressing process, a protrusion is produced on the obverse side, so the dimpled and protruded surfaces have to be investigated as heat transfer enhancement techniques. Numerical and experimental studies of heat transfer from such surfaces have mostly concentrated on analysing the flow structure and enhancement of heat transfer in turbulent flows, for example Belen'kiy *et al*, Ekkad *et al*, Mahmood *et al*, and Terekhov *et al*. [3-7]. However, recently much effort is being extended on developing nano, micro and mini devices, [8-10] so that heat exchangers involving laminar flow are now also of significant interest. Regrettably, the literature on laminar flows over dimpled and/or protruded surfaces is limited.

In order to be able to design optimal heat transfer surfaces consisting of array of dimples and/or protrusions, the flow and thermal fields around an isolated structure need to be understood first and then combined with combinations of dimple/protrusion as the next step.

Laminar flow structures over a single spherical dimple on an isolated flat plate with a rounded edge in semi-infinite domain were studied numerically by Isaev *et al* [11, 12] with

**Eddie Leonardi passed away on December 14, 2008.

the dimple Reynolds number, Re_D , range $100 < Re_D < 2500$, in which $Re_D = U_\infty D/\nu$, and D is the dimple imprint diameter, U_∞ is the velocity outside the boundary layer and ν is the kinematic viscosity. Unfortunately, there is no mention of either the position of the dimple along the plate or, what is equivalent, the Reynolds number based on the distance from the leading edge, x , viz, $Re_x = U_\infty x/\nu$. Instead, Isaev *et al* [11, 12] used the thickness of velocity boundary layer equal to the dimple depth, h , and the Polhausen velocity distribution as the boundary condition at the inlet of their calculation domain, which was located $5D$ upstream of the dimple centre. This approach reduces the region over which numerical calculations needed to be performed. However, using Polhausen velocity distribution as the inlet boundary condition leads to overshoots in the boundary layer downstream as shown by Alshroof *et al* [13], so that the results presented by Isaev *et al* [11, 12] may not be valid.

In order to obtain reliable results, Alshroof *et al* [13] showed that a much more thorough approach is necessary in terms of mesh refinement and boundary conditions, than that used by Isaev *et al* [11, 12]. As a consequence, Alshroof *et al* [13] found that in the range of $700 \leq Re_D \leq 3000$ the total heat transfer from the surface with a single dimple is reduced below its values on a smooth flat plate. Interestingly, despite the reduction in the overall heat transfer rate found by Alshroof *et al* [13], because there is a reduction in the shear stress over the dimple, the thermal performance factor, (defined as the ratio of the enhancement of heat transfer rate relatively to a smooth channel), over the change in the average shear stress, is marginally increased by a maximum of approximately 4%.

Khalatov *et al* [14], studied experimentally and numerically the flow structures and heat transfer within, and downstream of single spherical and cylindrical dimples. In particular, they investigated a shallow dimple with depth to imprint diameter ratio, h/D , equal to 0.1, in laminar and turbulent flows in the range $3,000 < Re_D < 23,600$. In the laminar regime they found that, the ratio between the heat transfer coefficients on the plate with the dimple decreased immediately downstream of the dimple. From $0.5D$ to $2.38D$ downstream of the dimple, the ratio increased to a maximum, then reduced so that at around $5-6D$ downstream the dimple, the effect of the dimple was no longer discernable. This is in general agreement with the results obtained by Alshroof *et al* [13], but it is not clear whether Khalatov *et al* [14] found that at the lower Reynolds numbers there is also a reduction in the overall heat transfer.

The problem of the dimple and protrusion heat transfer enhancement is changed by the introduction of boundaries, such as may be found in heat exchangers. Ligrani *et al* [15] experimentally studied the flow structures and local Nusselt number development in a rectangular channel with dimples on one wall and protrusions on the opposite wall. The dimples and protrusions were placed on the wide walls of the channel. Four relative offset positions were studied between dimples in one surface and protrusions on the other. The ratio of channel height to dimple and protrusion print diameter was 0.5, with a dimple and protrusion depth to print diameter of 0.22, and the channel Reynolds number, $Re_H = U_\infty H/\nu$, was varied in the range $380 < Re_H < 30,000$, in which H is the channel height. In each case, the presence of protrusions had a significant impact on flow structure and heat transfer. They claimed that six vortex pairs were present downstream of each dimple

protrusion combination, and a large proportion of flow was forced into dimple cavities, resulting in significant mixing even at low Reynolds numbers. This led to a considerable augmentation of local heat transfer over the dimpled surface. Unfortunately, the pressure drop was increased by a factor between 2 and 2.7 of that which pertained when a flat surface was used opposite the dimpled wall. This result might have been expected since there appears to be no heat transfer through the protrusion which, whilst acting to enhance the heat transfer in the dimples are also significant obstructions to the flow without themselves taking part in the heat transfer process. Therefore it appears to be an unfair judgment as to the merit of the effects of protrusions.

Similarly, Leontiev *et al* [16] studied the flow and heat transfer in channels with spherical dimples and proposed 'models' of flow separation in the laminar regime which were functions of the dimple parameters and Re_h , the Reynolds number based on the dimple depth. As Re_h is increased, the flow appears to separate with the formation of the symmetric vortices about the central axial plane of the dimple. Further increasing Re_h led to an increase in the length of the recirculation zone. Toroid-like vortices were observed.

Leontiev and his co-workers [16, 17] claimed that heat transfer is significantly increased with dimples in a channel in the same Reynolds number range as that studied by Alshroof *et al* [13]. They also found that dimples increases the pressure drop. This is in sharp contrast to Alshroof *et al* [13] who found that a dimple in a flat plate over cooled by a flowing fluid in a semi infinite region reduces the heat transfer rate as well as reducing the average shear stress on the plate.

Mahmood *et al* [6] extended the works of Ligrani *et al* [15] by investigating three configurations of dimple-protrusion in a channel in which dimples were located at one surface and flat, misaligned or aligned protrusions on the opposite surface. The channel aspect ratio was equal to 16, the channel height to dimple print diameter was 0.5, and dimple depth to dimple print diameter was 0.2 where the dimple diameter was 5.08 cm . The same values were used for protrusions. The Reynolds number based on channel height was in the range from 5×10^3 to 3.5×10^4 . The authors indicated a reduction in average heat transfer enhancement with increasing Reynolds numbers when protrusions were placed on the opposite wall, whilst in the case of the smooth opposite surface a change in average heat transfer was less dependent on Reynolds number. The increase of the thermal performance parameter by replacing the flat surface with protruded one, varied from 1.45 to 1.55 depending on the value of Reynolds number.

Wang *et al* [18] studied laminar flow in a $1D$ high, $1.62D$ wide and $8D$ long channel with a dimple placed in the centre of the bottom surface of the channel. A parabolic velocity profile was imposed at the inlet boundary, with an outflow boundary condition at the outlet, in the span-wise direction periodic boundary condition was employed. Two parametric ratios of dimple depth to its print diameter were investigated, 0.1 and 0.2, with dimple placed at the middle of the computational domain. They investigated the effect of Reynolds number, based on the maximum velocity and channel height on the flow separation in and around the dimple. No separation below $Re=100$ "based on maximum velocity" was observed. The flow separates at $Re>100$ and the separation region grows as the Reynolds number increases. These results qualitatively match

the results of many researchers including those of Isaev *et al* [11] and Alshroof *et al* [11-13].

A situation which appears to be of more general interest was investigated by Hwang *et al* [19] who experimentally studied the heat transfer and pressure drop in a rectangular channel with various combinations of dimpled, protruded and dimpled-protruded on the opposite wide walls of the conduit. The channel Reynolds number based on the hydraulic diameter was, in each case, fixed at 10^4 . Similarly to the results obtained by Alshroof *et al* [13], Mahmood *et al* [6] and Ligrani *et al* [15], a high heat transfer region was observed on the back surface of the dimple whereas, because of the separation, the remainder of the dimple surface had a low heat transfer flux. For the protruded surface, horseshoe vortices were generated thereby enhancing heat transfer on the front surface of the protrusion. On the other hand, a low heat transfer region existed on the back surface of the protrusion due to the wake downstream of the obstacle. The highest heat transfer flux occurred on the protruded surface, but, as may have been expected, this was also the area of maximum shear stress. As a consequence, the dimpled surface had the highest performance factor.

Hwang *et al* [19], studied the effect of various arrays of dimples, protrusion and combination of both in turbulent flow. They found that there was an increase in pressure drop when dimpled surfaces were tested. In laminar flow Alshroof *et al* [13] found that the shear stress over a single dimple on a flat plate is less than on the same position on a flat plate, leading to a small reduction in the drag on the whole plate. This implies that an array in laminar flow should lead to a reduction in the pressure drop.

One of the problems in discussing the flow around objects is to adequately describe the flow field. This is particularly difficult if the flow is unsteady such as that described by Acarlar and Smith [20], but even when the flow is steady it is a challenging task, as discussed by Alshroof *et al* [21]. They studied numerically the flow structure and heat transfer in a shallow channel with a single small protrusion. They found that the flow field downstream of the protrusion was very complex, consisting of interacting vortices which lead to complicated motions of fluid streams around the protrusion. The heat transfer flux distribution shown in Figure 1 can only be explained once the flow had been fully described. There was a significant increase in heat transfer in the vicinity of the protrusion accompanied by a small rise in pressure drop.

Despite all the above work, there is contradictory data based on differently defined Reynolds numbers, so that the information is insufficient for determining whether dimpled or protruded surfaces enhance heat transfer in heat exchangers, particularly in small channels in which the flow is likely to be laminar. There is only a small increase, in fact, possibly a decrease in the heat transfer rate when dimples are used in an attempt to enhance heat transfer in laminar flows.

Consequently, protrusion appears to show more promise, in spite of a likely increase in pressure drop. A numerical study was therefore undertaken in the laminar regime on the flow and heat transfer in a rectangular channel in which an isolated protrusion, an isolated dimple and combinations of a protrusion and a dimple were studied as a first step to obtaining adequate information for the development of heat exchangers employing protrusions to enhance heat transfer.

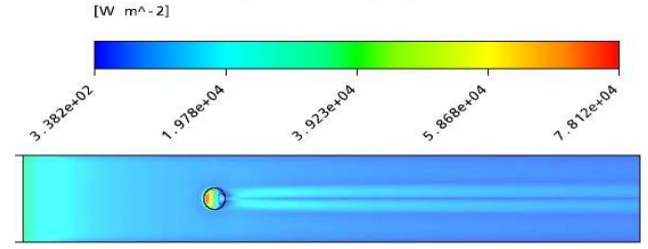


FIGURE 1 HEAT FLUX DISTRIBUTION ALONG THE CHANNEL WITH A PROTRUDED SURFACE [21].

SIMULATION METHODOLOGY

Three-dimensional computations of laminar incompressible flow were performed for the configuration shown in Figure 2. The flow and heat transfer were modeled by solving the three conservation equations for a fluid with constant properties, namely, the equation of continuity,

$$\nabla \cdot \mathbf{V} = 0, \quad (1)$$

the Navier-Stokes equation,

$$\rho \frac{\partial \mathbf{V}}{\partial t} + \rho \nabla \cdot (\mathbf{V}\mathbf{V}) = -\nabla p + \mu \nabla^2 \mathbf{V} \quad (2)$$

and the energy equation,

$$\rho c_p \frac{\partial T}{\partial t} + \rho c_p \nabla \cdot (\mathbf{V}T) - k \nabla^2 T = 0 \quad (3)$$

in which, ρ , c_p , \mathbf{V} , p , μ , ∇ , T , k , and t denote density, specific heat, velocity vector, gauge pressure, dynamic viscosity, gradient operator, absolute temperature, thermal conductivity and time respectively.

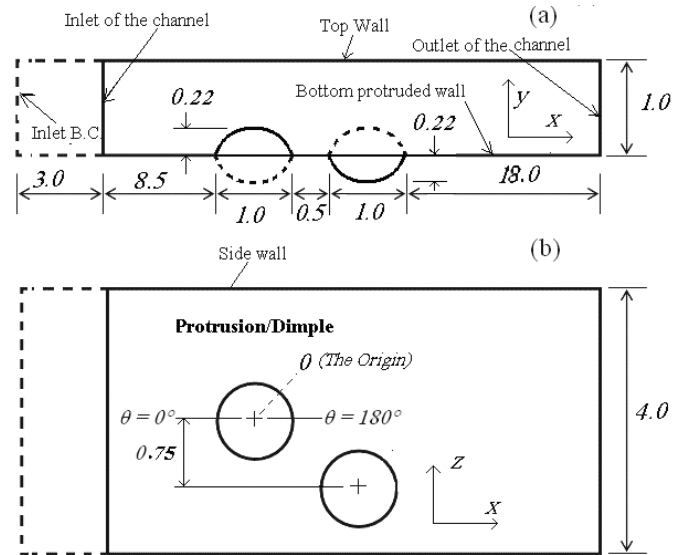


FIGURE 2 SCHEMATIC DIAGRAM OF COMPUTATIONAL DOMAIN, FOR PROTRUSION/DIMPLE CASE OR DIMPLE/PROTRUSION CASE; (A) ELEVATION AND (B) PLAN VIEWS. ALL LENGTHS ARE NON-DIMENSIONLIZED BASED ON THE PRINT DIAMETER OF THE OBSTACLE D .

BOUNDARY CONDITIONS

The sidewalls were modelled as adiabatic, whereas the top and bottom walls were set at a constant temperature of 45°C , with no slip wall boundary condition applied to all channel walls. A constant velocity profile of 1 ms^{-1} together with a constant temperature of 20°C and zero average gauge pressure were imposed at the inlet to the domain which was shifted $3D$ upstream of the channel entrance as is shown in Figure 2. A constant mass flow rate was set as the outlet boundary condition.

Adiabatic and zero shear stress conditions were imposed on all four bounding surfaces between the inlet to the computational domain and actual channel entry. The origin of the (x, y, z) coordinate system (Figure 2) of the geometry was located at the centre of the protrusion print diameter on the lower channel surface and is marked as θ in Figure 2(b).

SOLUTION METHOD

The problem was solved by obtaining the steady state temperature and velocity fields in the channel by using a commercial package, ANSYS CFX-11.0. A second order backward Euler differencing scheme was used for the transient term, and a second order upwind differencing scheme was employed for the advection terms in the Navier-Stokes equation. If the flow around the protrusion was steady, the solution was assumed to have converged when the residuals of all equations had been reduced to 10^{-8} . However, if the flow around the obstacle was unsteady, internal iterations were continued until the mass, momentum and energy residuals had been reduced to 10^{-6} at each time step. In order to determine whether the flow was steady or not, a transient calculations are performed.

DETAILS OF THE GRID

A combination of two types of grids has been used to discretise the equations. Firstly, an O-grid centered on the protrusion as well as the dimple and enclosing area of about $2D$ in diameter is presented in plan view in Figure 3. A very fine "body fitted" mesh was employed perpendicular to the bottom wall and protrusion surfaces. Secondly, a hexahedral grid was used in the remainder of the computational domain. The grid was concentrated over the protrusion and its surrounds so as to adequately resolve the complex flow structures around the protrusion. All lengths in this paper are expressed in obstacle print diameter D . The total number of grid points was 3.28×10^6 , 3.18×10^6 , 3.95×10^6 and 3.97×10^6 for single dimple case, single protrusion case, dimple upstream of protrusion case and protrusion upstream of dimple case respectively (Figure 3). With a time step of $7 \times 10^{-5}\text{ s}$ the solution converged to steady values on each of the meshes used. The converged solutions were then disturbed but, after going through a transient period, a steady flow was again predicted which differed by only a small fraction of a percent from the earlier results.

A grid convergence study was undertaken for a single protrusion case in order to choose an appropriate mesh size. Velocity values at the point $(7, 0.15, 0)$ and heat flux at a point on the protrusion surface at $(0, 0.22, 0)$ as a function of number

of grid cells are plotted in Figure 4. It can be seen that, when 3.18×10^6 grid cells were employed, the velocity and the heat flux had very nearly reached their asymptotic values, therefore, the results obtained with this mesh were assumed to be sufficiently accurate.

Now that the problem has been fully defined, and an appropriate mesh has been chosen, it is possible to discuss the results which have been obtained.

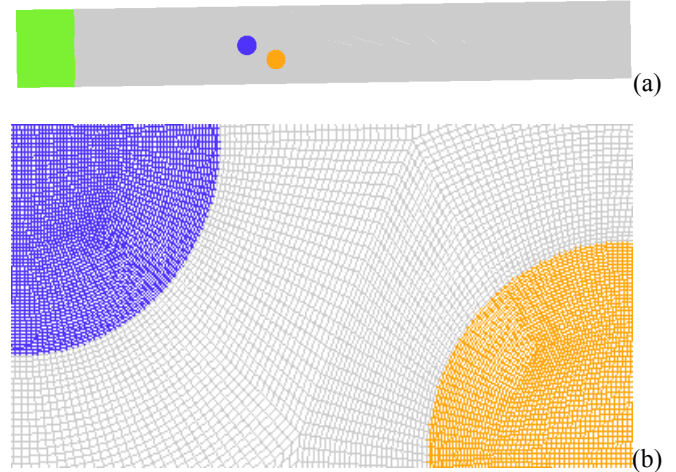


FIGURE 3 PLAN VIEW OF THE MESH ON THE PROTRUSION/DIMPLE PLANE FOR (A) FULL CHANNEL AND (B) ENLARGED VIEW NEAR PROTRUSION/DIMPLE.

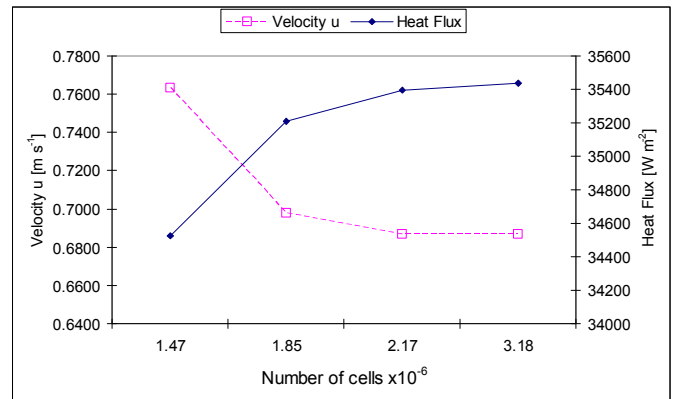


FIGURE 4 GRID CONVERGENCE STUDY FOR VELOCITY AT POINT LOCATED $(7, 0.15, 0)$, AND HEAT FLUX AT POINT LOCATED $(0, 0.22, 0)$ AS A FUNCTION OF NUMBER OF CELLS.

RESULTS AND DISCUSSION

In order to understand the interactions between heat enhancement devices, it is first necessary to appreciate the flow and heat transfer in each case individually. Once this has been completed, the flow and heat transfer for combinations of enhancement devices can be investigated and the changes wrought by various arrangements understood in terms of modification of the flow field, so that an optimal arrangement can be designed so as to minimize the pressure drop while maximizing the heat transfer. The results for a single dimple are

presented first, followed by isolated protrusion and then combination of them.

The following results are at channel Reynolds number of 1600.

Single Dimple

Since the dimple has a sharp edge where it intersects the plate, the flow separates from this edge with the fluid entering the separated region behind the centre of the print diameter starting approximately $0.1D$ from the vertical center plane of the channel. The stream forms an outward spiraling vortex, the centre line of which is slightly inclined to the horizontal. Some of the fluid which enters the dimple is ejected over the rear of the cavity as demonstrated by the yellow stream in Figure 5, most of the fluid remains in the vortex as is shown by the black stream in Figure 5. When this fluid reaches the edge of the dimple it is forced back into the dimple this time, spiraling near the centre of the vortex towards the axial centre plan of the dimple. Here it spirals outward and is ejected at the rear of the dimple.

Because of the separation in the dimple, the net affect is a slight reduction in the pressure drop required to maintain the flow in the channel.

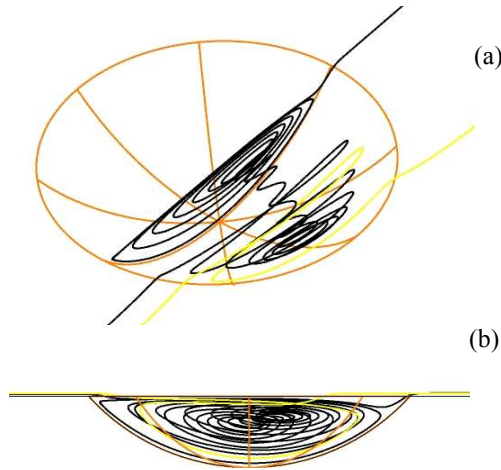


FIGURE 5 VORTEX WITHIN THE CAVITY WITH FLOW BEEN EJECTED FROM EITHER THE SIDE OF DIMPLE “YELLOW STREAM”, OR FROM THE DIMPLE CENTRE “BLACK STREAM”, (A) ISOMETRIC VIEW AND (B) SIDE VIEW.

The heat transfer distribution on the lower surface of the duct, within and downstream of the dimple, is shown in Figure 6. Regions of high heat transfer as well as areas of low heat transfer are evident and can be explained by the flow structure over and in the dimple. Since the flow entering the cavity is close to the surface and therefore relatively hot as shown in Figure 7a, and since the fluid in the vortex is “trapped” in the cavity, the fluid becomes quite warm thereby reducing heat transfer between it and the fluid above it, as is presented in Figure 7(b). When the trapped fluid reaches the centre plane of the dimple and spirals outward, significant heat transfer occurs as it is cooled by the fluid above it may also be seen in Figure 7(b). After that the slightly warmed fluid “hits” the trailing edge of the dimple causing a region of high heat transfer which continues for a distance downstream, as is

shown in Figure 6. This is in general agreement with the work of Khalatov *et al* [14].

On the other hand, the fluid which moves towards the transverse side of the dimple in the very tight spiraling vortices is quite hot when it reaches those edges so that there are regions of low heat transfer in the vicinity of the transverse edge of the dimple as is shown in Figure 7(c). The centre of the dimple is area of relatively high heat transfer. This outcome is due to the inclination of the vortex, and the relatively high velocities in the region.

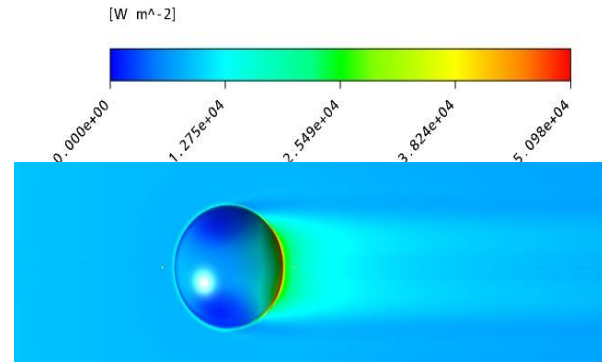


FIGURE 6 HEAT TRANSFER DISTRIBUTION OVER DIMPLED SURFACE.

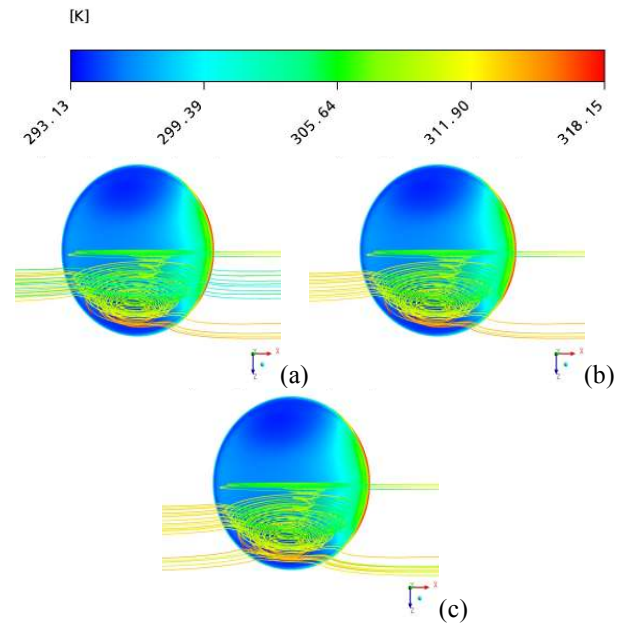


FIGURE 7 HEAT TRANSFER DISTRIBUTION OVER DIMPLE WITH (A) VORTEX IN THE CAVITY, (B) VORTEX WITH FLOW MOVING OVER IT, (C) VORTEX WITH FLOW MOVING OVER DIMPLE SIDE. ALL STREAMS ARE COLORED BY TEMPERATURE.

In agreement with Alshroof *et al* [13], in the dimple itself the heat transfer is in fact lower by a tiny 1%, than that which pertains in a smooth channel over at the same projected area. There is an increase in the heat transfer downstream of the dimple. Over an area defined by $-D \leq x \leq 10D$ and $D \leq z \leq D$ the heat transfer is increased by only 7.6%. This is

enormously lower than the threefold augmentation mentioned by Leontiev *et al* [17] and despite many attempts at reconciling these contradictory results, no satisfactory explanation has been found. Since it appears that the heat transfer enhancement by a dimple is rather small, the effect of replacing it by a protrusion was investigated.

Single Protrusion

The effect of a single protrusion is discussed in details by Alshroof *et al* [21], who showed there was a large increase on heat transfer on the protrusion it self and further downstream as maybe seen in Figure 8 in more detail than in Figure 1. There is also an increase in heat transfer for a significant distance downstream of the protrusion. Significantly this enhancement is confined into two well defined regions on either side of the axial vertical centre plane of the channel. The complex flow field downstream of the protrusion which leads to this phenomenon is discussed in detail by Alshroof *et al* [21] and will not be repeated here.

Unfortunately, the increase of heat transfer is accompanied by an increase in pressure drop [21] resulting in a performance factor *increase* of 33% in the vicinity of the protrusion. Once again there appears to be contradiction with the work of Leontiev *et al* [16] who indicate in their (Figure 1) that the performance factor is *decreased* when a protrusion is introduced in the channel. Similarly to the case of the dimple mentioned above, the reasons for this difference have not been established. Since the arrays of heat enhancement devices are required on heat exchanger without unduly increasing the pressure drop, the combination of a dimple on the centre line of the channel upstream of an off-centre protrusion or an arrangement with the position reversed was therefore investigated. The dimple upstream of the protrusion is discussed first.

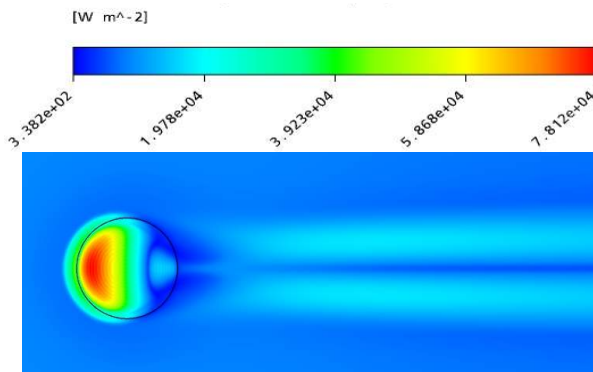


FIGURE 8 HEAT FLUX DISTRIBUTION OVER A PART OF THE PROTRUDED SURFACE [21]

Dimple Upstream of Protrusion

The flow structure over the dimple is entirely different in this case to the flow structure over a single dimple as may be seen by comparing Figure 9 with Figure 5. In Figure 9 fluid enters the cavity from one side of the dimple closest to the protrusion and is ejected from the other side near the channel sidewall. The fluid colored pink enters the dimple from a shallow region $0 < y \leq 0.03D$ with a horizontal extent from

$0.1D \leq z \leq 0.55D$. The stream below $0.03D$, which is colored yellow in Figure 9(a), also enters the dimple, but is trapped within the core of the vortex, and leaves the dimple with the fluid which was initially above it, now below it, as is shown in Figure 9(b).

Like the isolated dimple, there are regions of low heat transfer shown in Figure 10 on the transverse sides of the dimple which are caused by the relatively hot fluid entering the dimple as may be seen in Figure 11(a). The fluid which flows over the vortex in the dimple impinges on the rear of the dimple creating a region of high heat transfer. It is then reflected and moves to the side of the dimple as may be seen in Figure 11(b) leading to a low heat transfer region on the transverse side of the dimple away from the protrusion.

The low heat transfer region diametrically opposite the last mentioned area is caused by the fact that, as shown in Figure 9, the yellow high temperature stream enters here before it moves towards the axis of the vortex. Superficially, the regions of low heat transfer in Figure 10 and Figure 6 look similar, but the mechanisms are quite different.

As a consequence a relatively cooler fluid is in the proximity of the dimple wall. Together with the fact that there is no separation in the dimple, this leads to a significant increase of 26% in heat transfer over that which occurs in an isolated dimple.

On the other hand, the presence of the dimple has a minor effect on the flow structure around the protrusion. As may be seen in Figure 12, there is an asymmetry in the flow about the protrusion downstream of the dimple which is not seen when the protrusion is isolated [21]. This flow structure has a slight effect on the heat transfer rate distribution on the protruded surfaces, as shown in Figure 10 and Figure 11.

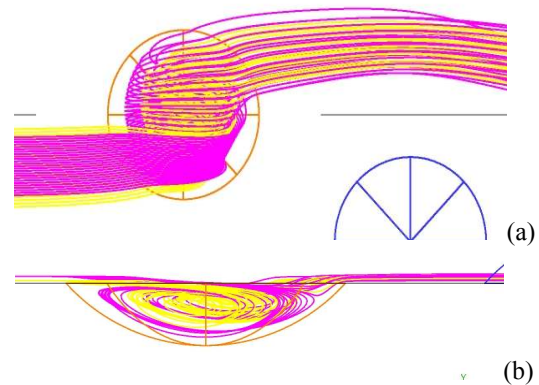


FIGURE 9 FLOW STRUCTURE WITHIN THE DIMPLE CAVITY, YELLOW STREAMS ARE AT LOWER LEVEL THAN THE PINK STREAMS, (A) TOP VIEW AND (B) SIDE VIEW.

The high heat transfer area downstream of the dimple is significantly distorted by the presence of the protrusion, as seen in Figure 10. Here, the heat transfer enhanced area downstream of dimple is not located on the dimple centre line as it is shown in Figure 6 for an isolated dimple, but is shifted toward the protrusion. The asymmetry caused by the fluid entering the dimple from one side, shown in Figure 9, Figure 11 and Figure 12, means that the fluid moving over the top of the vortex encounters less resistance over the half nearest the

protrusion, cooling this portion cavity more than the half away from the protrusion as is readily seen in Figure 10. As a result the “wake” is now shifted towards the protrusion and with it, as shown in Figure 11 and Figure 12, the high heat transfer area.

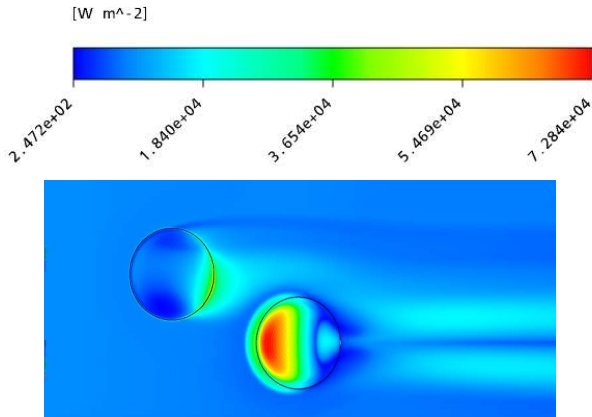


FIGURE 10 HEAT FLUX DISTRIBUTION IN THE VICINITY OF THE DIMPLED AND PROTRUDED SURFACE

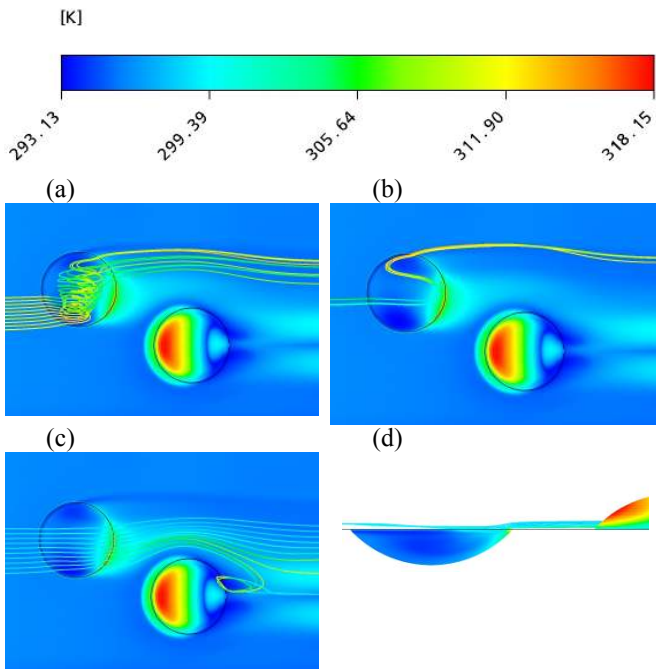


FIGURE 11 HEAT FLUX DISTRIBUTION ALONG THE DIMPLED PROTRUDED SURFACE, WITH (A) A STREAM OF FLOW AT LOW LEVEL UPSTREAM THE DIMPLE, (B) A STREAM OF HOT FLOW EJECTED FROM DIMPLE CAVITY, (C) A STREAM OF FLOW AT HIGHER LEVEL UPSTREAM THE DIMPLE WHICH MOVES OVER THE DIMPLED VORTEX AND (D) SIDE VIEW (C).

The fluid in the wake which flows around the protrusion and the wake from the dimple are then incorporated into the wake from the protrusion.

Despite the asymmetry and the presence of the high heat transfer region downstream of the dimple, there is little change in the heat transfer distribution on and downstream of the protrusion from that which pertains on an isolated protrusion as may be seen in Figure 13. In fact, there is a only tiny, less that

1%, change in the overall heat transfer rate on the protrusion surface downstream of the dimple relative to that which occurs on an isolated protrusion.

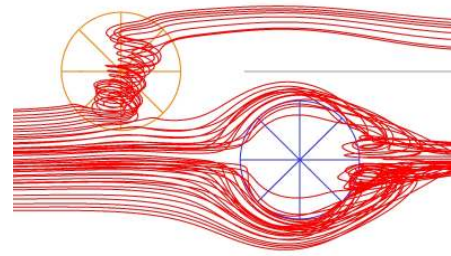


FIGURE 12 ASYMMETRIC FLUID AROUND AND DOWNSTREAM THE PROTRUSION CENTERLINE, WITH SOME FLUID BEEN DRAGGED INTO THE DIMPLE CAVITY.

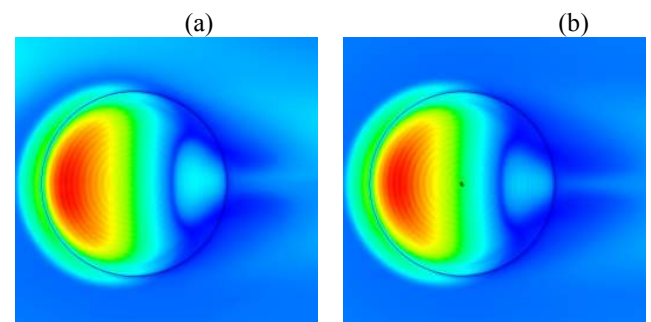


FIGURE 13 HEAT FLUX DISTRIBUTION OVER PROTRUSION SURFACE (A) SINGLE PROTRUSION CASE AND (B) DIMPLE UPSTREAM THE PROTRUSION.

Since this paper describes a preliminary study to those involving arrays of heat transfer enhancing devices, the reversal of positions of the dimple and protrusion are examined next.

Protrusion Upstream of Dimple

The fluid structure over an isolated protrusion is very complex [21], and it seems to be significantly affected by the presence of the downstream dimple, as may be seen in Figure 14, yet surprisingly once again there is no change in the total heat transfer on the protrusion in this case, from that of an isolated protrusion. However, there is an increase of 36% in the overall heat transfer rate in the dimple over that obtained from an isolated dimple and an enhancement of 10% over the heat transfer rate attained in the dimple when it is upstream of the protrusion. The reasons for this increase in the heat transfer rate are somewhat similar to those which caused the increase in heat transfer when the dimple was upstream of the protrusion as is shown in Figure 15 and Figure 9. However, this time the fluid which enters the cavity is at a higher level as may be seen by comparing Figure 15(b) with Figure 9(b). Since the fluid entering the dimple when it is downstream of the protrusion, is initially further away from the wall, it is cooler than the fluid which entered the dimple when it was upstream of the protrusion, so that there is an increase in heat transfer in the dimple when it is downstream of the protrusion over that when it is upstream of the protrusion.

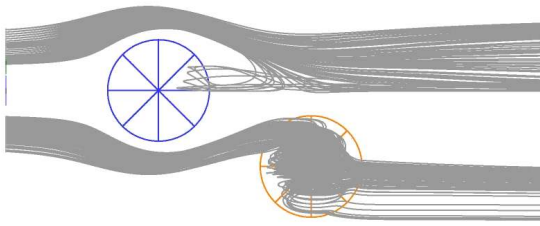


FIGURE 14 STREAM OF FLUID WHICH ENTERS TWO OPPOSITE UPSTREAM REGIONS OF PROTRUSION.

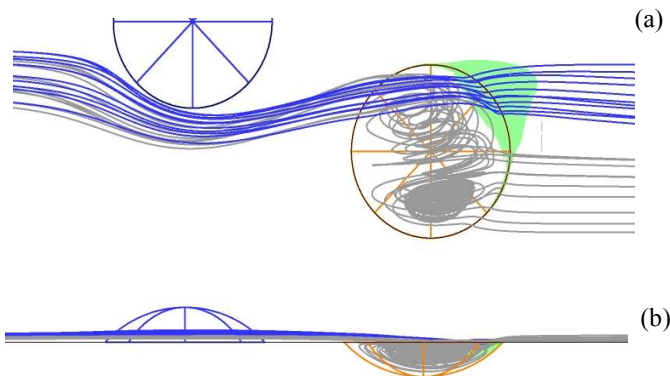


FIGURE 15 FLUID (COLORED BY GRAY) ENTERS THE DIMPLE CAVITY, AND (BLUE) STREAM ABOVE IT TOGETHER WITH AREA OF IMPINGEMENT COLORED BY GREEN, (A) TOP VIEW AND (B) SIDE VIEW.

The heat transfer distribution over the protruded surface shown in Figure 16(a) is the same as that over a single protrusion as may be seen in Figure 8. Areas of high heat transfer within and down stream of the dimple, as well as areas of low and high heat transfer within the dimple cavity are presented in Figure 16.

As presented in Figure 14 and Figure 15, the cool fluid shown in grey moving near the protrusion enters the dimple cavity and forms a vortex which eventually exits at high temperature over half of the trailing edge of the dimple nearest to the side wall. The vortex nearest the wall is shown in Figure 17. Another stream of fluid shown in blue in Figure 15, is initially at a higher level than the fluid stream marked in grey and is therefore cooler than it. However, under the influence of the vortices shown in Figure 17 the fluid marked in blue is forced to move towards the sidewall and because the fluid marked in grey is drawn into the dimple, the cold fluid marked in blue is brought near the lower surface downstream of the dimple. A portion of this fluid impinges on the rear of the dimple marked by the green area in Figure 15 over the half away from the side wall, thereby creating a region of higher heat transfer as may be seen in Figure 16.

Once again, as may be seen in Figure 16, there are two almost diametrically opposite areas of low heat transfer within the dimple. These are the result of two very tight portions of the spiraling vortex, one of which is clearly seen Figure 15.

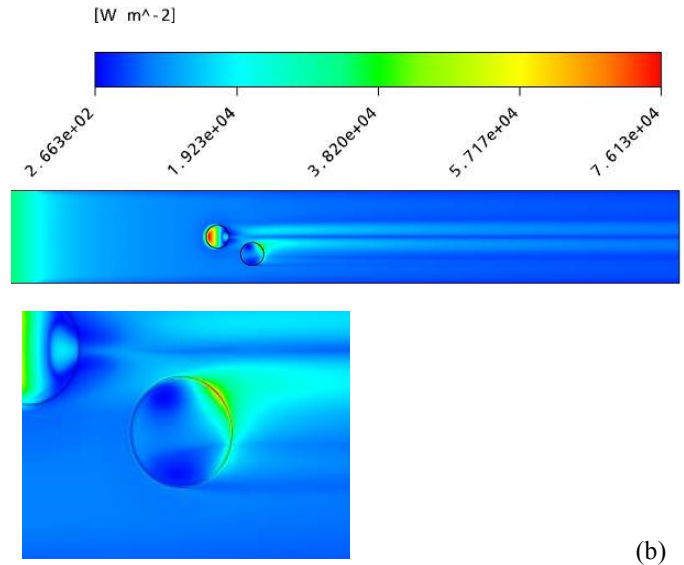


FIGURE 16 HEAT FLUX DISTRIBUTION ALONG (A) THE BOTTOM SURFACE AND (B) ENLARGED OVER THE DIMPLE CAVITY.

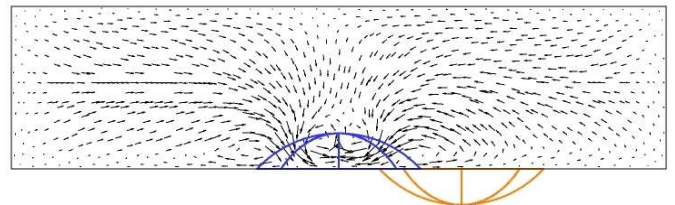


FIGURE 17 CROSS SECTIONAL VELOCITY VECTORS, LOCATED AT Y-Z PLANE AT 2.5D DOWNSTREAM OF THE ORIGIN.

While it is clear that all four schemes examined above lead to an increase in heat transfer, some means of evaluating the effectiveness need to be developed.

EFFECTIVENESS OF THE ENHANCEMENT

One of the common methods of heat transfer augmentation is to increase the surface area exposed to one of the fluids involved in a heat exchanger; for example when fins are introduced in a car radiator. It is therefore necessary to show that any proposed scheme involving an increase in area leads to a significant increase in a heat transfer. If the augmentation in heat transfer is significantly greater than the increase in area, then the scheme has a great potential for use in heat exchangers. Further, if the resultant increase in heat transfer is greater than the usual concomitant increase in pressure drop, the arrangement is usually adjudged as being of significant value. These issues are discussed below.

Enhancement as a Function of Area

The effect of an increase in area can be considered in two ways, one concerns the change in heat transfer in the location at which the heat transfer occurs and the other is related to the total effect of change in area over the whole affected region.

The non-dimensional increase in area with the imprint area as the reference for the a dimple or the protrusion, A_i is given by

$$A_i = (2h/D)^2, \quad (4)$$

In which, $h/D = 0.22$, means that $A_i \approx 0.194$.

As may be seen in Figure 18, the change in heat transfer flux distribution from that in a smooth channel, caused by the presence of a dimple, over $2D$ wide strip centered at the bottom surface of the channel and it starts about $1D$ upstream of its centre and, for all practical purposes, ends $10D$ downstream of its centre. Although there is quite a large increase in the heat flux from that in a smooth channel down stream of $10D$ for the other cases shown in Figure 18, for consistency the length of the affected area will be taken as that for a single dimple; that is $11D$ long starting at $-1D$.

If the increase in heat transfer is less than the enlargement in the area, then it can be said that the area is not being effectively utilized. It follows that in terms of the effectiveness of an increase in area, the single dimple as shown in Figure 21, which leads to a slight decline in heat transfer, is not effective. However, since the heat transfer is augmented downstream of the dimple if the previously mentioned $2D$ wide strip is used then the increase in area, as a fraction of the total area involved, is only 0.7%. This means that the approximately 7% increase in heat transfer for single dimple is shown in Figure 20, has real merit in terms of the change in area.

Similarly, the increase in the area resulting from the introduction of a single protrusion is once again 19.4%, but the heat transfer, as may be seen in Figure 21, is a hard to believe, four times that which pertains in a smooth channel. Obviously in terms of an area increase the introduction of the protrusion, which leads to such an enhancement in heat transfer, is worthwhile. When taken over the same strip as that used above for determining the effectiveness of an isolated dimple, the increment in heat transfer, as given in Figure 20 is reduced to 36%; a respectable enhancement.

As mentioned above once a protrusion is introduced downstream of the dimple, whilst the heat transfer on the protrusion is not greatly changed, but the heat transfer in the dimple is increased, as a consequence whilst the total area of both structures together is again 19.4% larger than the print area they occupy, and as is shown in Figure 21, the heat transfer is 2.68 times that in a smooth channel.

Similarly, when the positions of the dimple and protrusion are reversed, once again as presented in Figure 21, the heat transfer is 2.75 times that which occurs in a smooth channel; a slight increase over the previous situation.

A staggered combination of protrusion downstream of a dimple, or a dimple downstream of the protrusion, results in a configuration shown in Figure 2. It follows that heat transfer distribution is changed as shown in Figure 10, Figure 11 and Figure 16, over a larger area than the strip used when discussing the isolated structures. Therefore, in this case area of $3D$ wide ($-1D \leq z \leq 2D$) and $11D$ long is used.

The relative heat transfer over the $3D$ wide area is increased by 26% over single protrusion, as shown in Figure 20. When combinations of a protrusion and a dimple are used, as may be seen in Figure 20, the relative heat transfer over the same area is increased by a further 5% and 6% depending whether the dimple or the protrusion is in the

upstream position. This is significantly grater than the 0.5% increase in area caused by using the combination of the obstructions, but whether the changes in pressure drop are also advantageous still needs to be determined.

Evaluation of enhancement in terms of pressure drop

The shear stress distribution averaged over the width of the channel on the surface containing the heat transfer enhancement structures is presented in Figure 19. Whilst there are very large increases in shear stress over the protrusion, followed by a drop in its value in the wake, there is a decrease in the shear stress over the dimple (D) followed by a rise immediately downstream. The net result is that there is very little decrease in the pressure drop when an isolated dimple is employed, but there is an increase in the pressure drop when a protrusion (P) is employed, which as may be seen in Figure 20 does not change significantly when a dimple (D-P or P-D) is also present.

A measure that has often been used to indicate, albeit imperfectly, the overall improvement in performance of a heat transfer device, is the performance index, f , defined as

$$f = (q'/\tau)/(q'_0/\tau_0), \quad (5)$$

in which q' and τ are the average heat flux and the average shear stress on the appropriate areas respectively, and the subscript 0 indicates the smooth channel.

Surprisingly, as may be seen in Figure 20, since the average shear stress, over the strip in which the single dimple is located, is 1.5% lower than that which occurs in a smooth channel, the average heat flux increase of 7% results in an f value of 1.09.

On the other hand the 36%, 31% and 32% enhancement of the average heat flux associated with the P, D-P and P-D combinations results in f values of 1.32, 1.3 and 1.3 respectively, as is shown in Figure 20. It should be noted that the small change in the values of f for the combination cases from that of the protrusion alone occur only because there is hardly any change in the average shear stress when a dimple is introduced in addition to the protrusion. However, because of the larger area used in averaging the heat flux, the net heat transfer increase is significantly greater when the dimple is introduced in addition to protrusion.

Whereas as the presence of a dimple in the side of a shallow channel enhances heat transfer by 7% and increases the performance factor by 9%, a protrusion and combinations of a dimple and a protrusion are significantly greater in both respects with the performance factor being increased by approximately 30%. If arrays of protrusions were used in a heat exchanger there would a large benefit in terms of heat transfer, but there would be a significant penalty in terms of pressure drop. The presence of arrays of dimples and protrusions might therefore be a good way of enhancing heat transfer in the laminar regime without inducing too great an increase in the pressure drop.

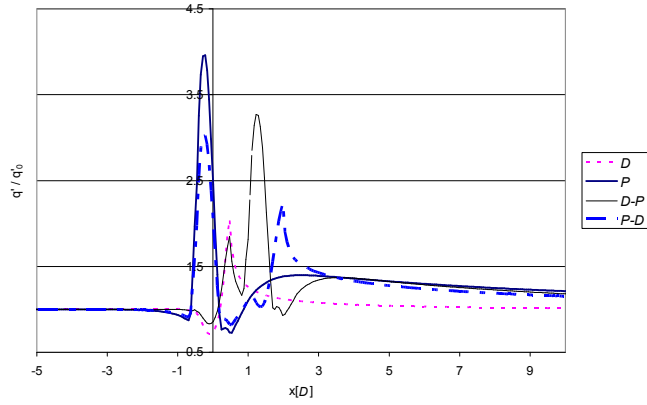


FIGURE 18 RELATIVE HEAT FLUX AS FUNCTION OF POSITION AT THE BOTTOM SURFACES AVERAGED OVER 2D WIDE STRIP FOR SINGLE PROTRUSION (P); SINGLE DIMPLE (D) AND AVERAGED OVER A 3D WIDTH FOR THE COMBINATIONS OF A DIMPLE - PROTRUSION D-P, AND A PROTRUSION - DIMPLE (P-D).

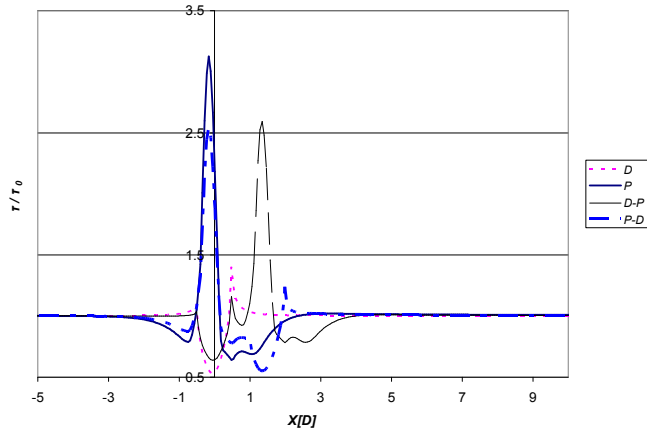


FIGURE 19 RELATIVE SHEAR STRESS AS FUNCTION OF POSITION FOR BOTTOM SURFACES AVERAGED OVER 2D WIDE STRIP FOR SINGLE PROTRUSION (P) AND SINGLE DIMPLE (D), AND AVERAGED OVER A 3D WIDTH FOR THE COMBINATIONS OF A DIMPLE - PROTRUSION D-P, AND A PROTRUSION - DIMPLE (P-D).

CONCLUSION

Three-dimensional computations have been performed to study the feasibility of using spherical protrusion-dimple combinations in a shallow channel for enhancing heat transfer at a channel Reynolds number of 1600.

Despite the decrease in the heat transfer in the dimple cavity below that which occurs at the same location in a smooth channel, there is an increase in heat transfer down stream of the dimple. This leads to an overall increase in heat transfer of 7%, which together with a reduction of 1.5% in the average shear stress on the area, results in an increase of approximately 9% in the performance factor.

Although a dimple leads to an augmentation in heat transfer, it is dwarfed by the five times increase in heat transfer obtained when a protrusion is used. Despite an increase in the average shear stress, this also leads to an increase of 32% in the performance factor.

The addition of a staggered dimple, either upstream or downstream of the protrusion, leads to a further increase in heat transfer without a concomitant rise in the average shear stress. However, because the heat flux is averaged over a larger area there is a small reduction in the performance factor to 1.3.

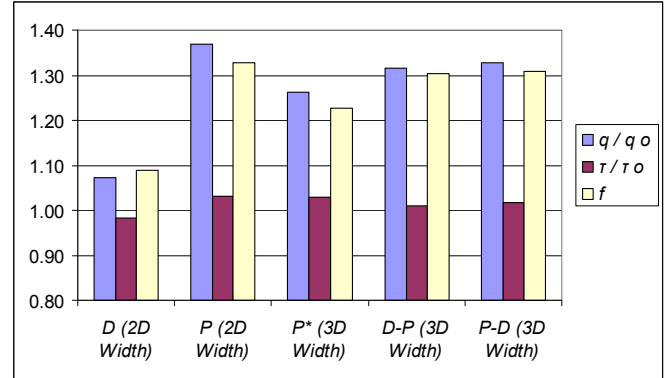


FIGURE 20 RELATIVE HEAT FLUX, RELATIVE SHEAR STRESS AND PERFORMANCE FACTOR AVERAGED OVER 2D WIDTH FOR SINGLE DIMPLE (D) AND SINGLE PROTRUSION (P); AVERAGED OVER A 3D WIDTH FOR THE SINGLE PROTRUSION (P*), COMBINATIONS OF A DIMPLE - PROTRUSION D-P, AND A PROTRUSION - DIMPLE (P-D).

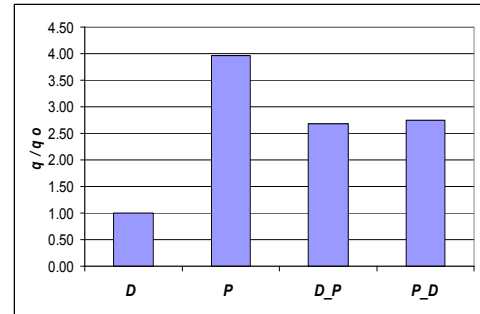


FIGURE 21 HEAT FLUX AVERAGED OVER THE OBSTACLE SURFACE RELATIVE TO THE AVERAGED HEAT FLUX ON THE PROJECTED AREA ON A SMOOTH CHANNEL, FOR SINGLE DIMPLE, SINGLE PROTRUSION, COMBINATION OF A DIMPLE-PROTRUSION AND A PROTRUSION - DIMPLE.

NOMENCLATURE

D	print diameter of the protrusion
h	height of the protrusion
H	height of the channel
W	Width of the channel
Re_D	Reynolds number = $D U_\infty / \nu$
Re_h	$Re_h = U_\infty h / \nu$
Re_H	$Re_H = U_\infty H / \nu$
Re_x	$Re_x = U_\infty x / \nu$
U_∞	free stream velocity upstream of the channel
u	velocity in the direction parallel to channel walls

v	velocity in the direction perpendicular to the bottom wall
w	transverse velocity
0	origin of coordinate system
0	indicates the smooth channel
x	coordinate in the direction parallel to channel walls
y	coordinate in the direction perpendicular to the bottom wall.
z	coordinate in the direction perpendicular to the side wall.

REFERENCES

- [1] Incropera, F. and DeWitt, D., *Introduction to Heat Transfer*. THIRD ed. 1996, Canada: John Wiley & Sons, Inc.
- [2] Mahmood, G. I., Hill, M. L., L., Nelson D., M., Ligrani P., Moon, H.-K., and B., Glezer, *Local Heat Transfer and Flow Structure on and above a Dimpled Surface in a Channel*. Trans. ASME, J. Turbomachinery, 2001. **123**(1): p. 115–123.
- [3] Mahmood, G. I. and Ligrani, P. M., *Heat Transfer in a Dimpled Channel: Combined Influences of Aspect Ratio, Temperature Ratio, Reynolds Number, and Flow Structure*. Int. J. Heat Mass Transfer, 2002. **45**(10): p. 2011–2020.
- [4] Belen'kiy, M. and Gotovskiy, M., *Experimental Investigation of Heat and Hydraulic Characteristics of Heat Transfer Surfaces Formed by Simi-Spherical Cavities*. High Temperature,, 1991. **29**(6): p. 1142–1147.
- [5] Ekkad S. V. and Nasir H., *Dimple Enhanced Heat Transfer in High Aspect Ratio Channels*. Journal of Enhanced Heat Transfer, 2003. **10**(4): p. 395–406.
- [6] Mahmood, G. I., Sabbagh, M. Z., and Ligrani, P. M., *Heat Transfer in a Channel with Dimples and Protrusion on Opposite Walls*. Journal of technology and heat transfer, 2001. **15**(3): p. 375–283.
- [7] Terekhov, V. I., Kalinina, S. V., and Mshvidobadze, Y. M., *Heat Transfer Coefficient and Aerodynamic Resistance on a Surface with a Single Dimple*. Enhanced Heat Transfer, 1997. **4**: p. 131–145.
- [8] Lukes, J., Abramson, A., and McGaughey, A., *Fundamentals of Heat Transfer in Micro/Nano Systems*, in *ASME Summer Heat Transfer Conference*. 2007.
- [9] Ho, Chih-Ming. and Tai, Yu-Chong., *MICRO-ELECTRO-MECHANICAL-SYSTEMS (MEMS) AND FLUID FLOWS*. Annual Review of Fluid Mechanics, 1998. **30**: p. 579–612.
- [10] KAWANO, K., SEKIMURA, M., MINAKAMI, K., IWASAKI, H., and ISHIZUKA, M., *Development of Micro Channel Heat Exchanging*. JSME International Journal Series B, 2001. **44**(4): p. 592–598.
- [11] Isaev, S., Baranov, P., and Usachov, A., *Numerical Analysis of the Effect of Viscosity on the Vortex Dynamics in Laminar separated Flow Past a Dimple on a plate with Allowance for its Asymmetry*. Journal of Engineering Physics and Thermophysics, 2001. **74**(2): p. 339–346.
- [12] Isaev, S., Leontiev, A., Usachev, A., and Frolov, D., *Numerical Simulation of Laminar Incompressible Three – Dimensional Flow Around a Dimple (Vortex Dynamics and Heat Transfer)*. Russian Ministry of Science and Technologies, Institute for High Performance Computing and Data Bases, 1997. **97**(6): p. 1–21.
- [13] Alshroof, O., Reizes, J., Timchenko, V., and Leonardi, E., *Numerical Evaluation of Heat Transfer from a Spherical Dimple in a Flat Plate: Development of Appropriate Boundary Conditions*, in *ASME International Mechanical Engineering Congress and Exposition*. 2007: Seattle, Washington, USA. .
- [14] Khalatov, A., Byerley, A., Ochoa, D., Min, S-K., and Vincent, R., *Application of advanced Techniques to Study Fluid Flow and Heat Transfer Within and Downstream of a Single Dimple*, in *Proceedings of V Minsk International Heat & Mass Transfer Forum*. 2004: Minsk.
- [15] Ligrani, P., Mahmood, G., Harrison, J., Clayton, C., and Nelson, D., *Flow Structure and Local Nusselt Number Variations in a Channel with Dimples and Protrusions on Opposite Walls*. International Journal of Heat and Mass Transfer, 2001. **44**(23): p. 4413–4425.
- [16] Leontiev, A., Gortyshov, Yu., Popov, I., and Olimp'ev, V., *Hydrodynamics And Heat Transfer in Heat Exchanger Channels With Spherical Holes*, in *ASME International Mechanical Engineering Congress & Exposition*. 2006: Chicago, Illinois, USA.
- [17] Leontiev, I., Olimp'ev, V., Dilevskaya, V., and Isaev, S., *The Nature of Heat Transfer Enhancement Mechanism on Surfaces with Spherical Holes*,. Izv. RAN, Energetika,, 2002. **2**: p. 117–135.
- [18] Wang, Z., Yeo, K., and Khoo, B., *Numerical Simulation of Laminar Channel Flow Over Dimpled Surface*, in *16th AIAA Computational Fluid Dynamics Conference*. 2003: Orlando, Florida.
- [19] Hwang, S.D. and Cho, H.H., *Heat transfer enhancement of internal passage using dimple/protrusion*, in *13th International Heat Transfer Conference*. 2007: Sydney, Australia.
- [20] Acarlar, M. S. and Smith, C. R., *A study of hairpin vortices in a laminar boundary layer. Part 1. Hairpin vortices generated by a hemisphere protuberance*. J. Fluid Mech, 1987. **175**: p. 1–41.
- [21] Alshroof, O., Reizes, J., Timchenko, V., and Leonardi, E., *Heat Transfer Enhancement in Laminar Flow by a Protrusion in a Rectangular Channel*, in *ICHMT International Symposium on Advances in Computational Heat Transfer*. 2008: Marrakech, Morocco.